Original Article
HLA-E inhibitor enhances the killing of neuroblastoma stem cells by co-cultured dendritic cells and cytokine-induced killer cells loaded with membrane-based microparticles

Zijun Zhen[1,2,3], Kaibin Yang[1,4], Litong Ye[1,4], Zhiyao You[1,4], Rirong Chen[1,4], Ying Liu[1,4], Youjian He[1,3,5]

[1]State Key Laboratory of Oncology in South China, Guangzhou, China; Departments of [2]Pediatric Oncology, [5]Medical Oncology, Sun Yat-sen University Cancer Center, Guangzhou, China; [3]Collaborative Innovation Center of Cancer Medicine, Guangzhou, China; [4]Sun Yat-sen University Zhongshan School of Medicine, Guangzhou, China

Abstract: Neuroblastoma stem cells (NSCs) can cause drug resistance and tumor recurrence. This study aimed to enhance the lytic effect of dendritic cells (DCs) co-cultured with cytokine-induced killer (CIK) cells. NSCs were obtained by suspension culture, and DC-CIK cells were loaded with extracted NSC membrane-based microparticles (MMPs) before evaluating the lytic effect of DC-CIK cells on NSCs. After inhibiting the function or expression of human leukocyte antigen-E (HLA-E) in NSCs by anti-HLA-E monoclonal antibody or siRNA, the DC-CIK cell lytic effect on NSCs was re-assessed. NSC nestin expression was high, but glial fibrillary acid protein expression and class IIIβ-tubulin-1 expression were low. Moreover, NSCs exhibited strong tumorigenic ability in nude mice. Loading DCs with NSC-derived MMPs induced the differentiation of DCs and CIK cells and enhanced the killing of NSCs by DC-CIK cells. Inhibiting the function or expression of HLA-E in NSCs further enhanced the cytolytic capability of DC-CIK cells loaded with NSC-derived MMPs. HLA-E inhibitor can enhance the killing of NSC by DC-CIK cells loaded with NSC-derived MMPs.

Keywords: Neuroblastoma, stem cell, immunotherapy, human leukocyte antigen, monoclonal antibody

Introduction

Neuroblastoma (NB) is an aggressive malignant tumor commonly seen in childhood, and the long-term survival rate of high-risk patients remains very low [1, 2]. Thus, novel approaches should be developed to enhance treatment outcome. In recent years, the tumor stem cell theory has been gradually emphasized in this context [3]. Specifically, neuroblastoma stem cells (NSCs) play a crucial role in the tumor invasion, drug resistance, and recurrence of NB [4, 5], and precise treatment targeting NSCs is likely to improve the outcomes of patients with NB. Dendritic cells (DCs) and cytokine-induced killer (CIK) cells have been increasingly applied in anti-tumor immunotherapy, which has become a novel modality in cancer treatment [6, 7]. Nevertheless, conventionally cultured DC-CIK cells lack targeted killing capability, leading to poor clinical efficacy [8].

Tumor antigen is a main source for obtaining DC-CIK cells with targeted killing ability [9]. At present, almost 1000 categories of tumor-associated antigens have been identified; however, most tumors lack effective tumor-specific antigens. Moreover, tumor cells are heterogeneous and likely to harbor mutations. Hence, immunotherapy targeting a single antigen has consistently proved ineffective [10]. Accordingly, a more complete panel of tumor antigens offers certain advantages, and complete tumor antigen-loaded DCs may represent an effective approach to obtain DC-CIK cells that target specific tumors [11].

The tumor cell membrane can release membrane-based microparticles (MMPs) with a capsular structure via froth exfoliation [12]. These MMPs carry multiple tumor antigens from the parent cells and can be effectively taken up by DCs via the classical endocytotic pathway

and degraded by the intracellular lysosome, which accelerates the DC presentation of tumor cell antigens [13, 14]. Therefore, NSC-derived MMPs could be used as a complete cell antigen complement to sensitize DCs and establish a highly specific and effective novel immunotherapy that targets NSCs, a technique that has not yet been reported.

Human leukocyte antigen-E (HLA-E), which is expressed on the surface of tumor cells, is a major ligand of the inhibitory receptor CD94/NKG2A of natural killer (NK) cells and cytotoxic T lymphocytes (CTLs), which represent one of the main mechanisms underlying tumor immune escape [15]. Moreover, HLA-E correlates with the unfavorable features of NB [16, 17]. T cells expressing CD3 and CD56 (CD3$^+$CD56$^+$T cells) are the main effector cells functioning among CIK cells [18]. Similar to other T cells, CD3$^+$CD56$^+$T cells also express CD94/NKG2A/B, ILT2/LIR1, KIR, and other inhibitory receptors. HLA-E expressed in tumor cells may inhibit the activity of CD3$^+$CD56$^+$T cells via these receptors and influence the anti-tumor effect of CIK cells [19]. In this study, NSC-derived MMPs were loaded onto DC-CIK cells to enhance their killing of NSCs. In addition, the influence of HLA-E inhibitor on this immunotherapy was evaluated.

Materials and methods

Ethical approval

All human samples were donated freely, and informed consent was obtained from all children/guardians. Ethical approval was obtained from the Institutional Review Board of Sun Yat-sen University in China and followed the Declaration of Helsinki principles [20].

Materials

Recombinant human epidermal growth factor, recombinant human basic fibroblast growth factor, and recombinant human leukemia inhibiting factor were purchased from Peprotech (NJ, USA). DMEM/F12 culture medium, 1640 culture medium, B27, and fetal bovine serum were bought from Gibco (NY, USA). A low-adherence culture flask was purchased from Corning (NY, USA). Mouse anti-human CD3, CD56, CD4, CD8, CD83, and CD86 were provided by BioLegend (CA, USA). A total RNA extraction kit,

RNA reverse transcription kit, and RT-PCR quantitative detection kit were purchased from Takara (Nagoya, Japan). The anti-HLA-E monoclonal antibody TFL-007 was supplied by the Terasaki Foundation Laboratory.

Primary culture

Primary cell culture was used to grow and expand NB cells isolated from two children with newly diagnosed NB; both patients had been diagnosed with stage IV disease according to the international NB staging system. One patient was a 2-year-old boy with a primary tumor in the left adrenal region and metastatic disease in his skeleton and bone marrow. The N-MYC gene was amplified in this tumor. The second patient was a 3-year-old girl with a primary tumor in the right adrenal region and metastatic disease in the posterior mediastinum and bone marrow. In this case, the N-MYC gene was unamplified. Neither patient had previously received chemotherapy or radiotherapy. Following the collection of a bone marrow specimen sufficient for clinical diagnosis, the remaining specimen was used for primary culture as previously described [21]. The cells obtained from these two patients were designated NB1 and NB2. HLA-E was highly expressed in the tumor tissues and primary cultured tumor cells, as detected by immunohistochemical staining [22] and western blot [23], respectively.

Suspension culture

NB1 and NB2 cells were cultured in DMEM solution containing 10% fetal bovine serum and incubated at 37°C in an atmosphere of 5% CO_2 and 90% relative humidity. A low-adherence culture flask was inoculated with cells at the logarithmic phase, and the suspension was cultured in an incubator. The culture solution was replaced with DMEM/F12 medium containing 20 ng/ml of basic fibroblast growth factor, 20 ng/ml of epidermal growth factor, 2% of B27, and 20 ng/ml of leukemia-inhibiting factor [24]. The cell concentration was adjusted to 1×10^5/ml. Half of the culture solution was replaced every 3 d, and the cells were passaged at a ratio of 1:3 every 7 d. The third and fourth generations of the cells inside the cell spheres were prepared for subsequent experiments.

Immunofluorescence

After 3 d of culture, NB1, NB2, and corresponding cells inside the cell spheres were collected. The cells were adjusted to a concentration of 1×10^8 cells/L and seeded in a 24-well culture plate with a cover slip. When the cells attached to the wall, they were fixed with paraformaldehyde for 10 min, washed with phosphate-buffered saline (PBS), and then washed with PBS containing 0.1% Triton X-100 before being blocked with 5% bovine serum albumin for 30 min at room temperature for 1 h. The cells were then incubated with nestin primary antibody for 2 h. The cells were washed in PBS and then incubated with Cy3-conjugated secondary antibody for 30 min in a dark room before being stained with 4', 6-diamidino-2-phenylindole. The cells were washed again in PBS, mounted after drying, and photographed under a fluorescence microscope.

Reverse transcription-polymerase chain reaction (RT-PCR)

Cells inside the NB1 and NB2 cell spheres were collected after being cultured for 3 days. Total RNA was extracted and reverse transcribed to cDNA using the following conditions: extension at 30°C for 10 min and annealing at 42°C for 30 min, followed by termination at 99°C for 5 min and cooling at 5°C for 5 min. The expression levels of the stem cell marker nestin, glial cell marker glial fibrillary acid protein (GFAP), and neuron marker class IIIβ-tubulin (Tuj-1) were detected by RT-PCR as previously described [25].

Animal model

The right armpits of nude mice were subcutaneously inoculated with third-generation cells from the NB1 and NB2 cell spheres at a density of 1×10^7 cells/mouse (n = 6 for each group), and equivalent quantities of NB1 and NB2 cells were injected subcutaneously into the right inguen as controls. The tumor formation time and rate of NSCs were observed. An emerging node at the inoculation site, as judged by macroscopic observation, represented tumor formation. The experiment was repeated three times, and animals were observed for 10 d. The nude mice were inoculated with NB1, NB2, and corresponding cells from the cell spheres at a density of 1×10^4 cells/mouse, and the above experimental procedures were repeated.

MMP extraction

Supernatant was collected after NSCs derived from NB1 and NB2 were cultured. The MMPs of NSCs were extracted by ultrafiltration and differential centrifugation methods and diluted with physiological saline for filtration and packaging. The concentrations of protein and nucleic acid were detected under ultraviolet light, and the quantity of endotoxin was evaluated using the *Tachypleusamebocyte* lysate test before storing the samples at -20°C according to previously described methods [26].

DC induction

Mononuclear cells were collected from the peripheral blood of volunteers, washed, centrifuged in physiological saline, re-suspended in 1640 culture solution, and then cultured at 37°C in 5% CO_2 for 2 h. The suspension cells were aspirated for subsequent CIK culture. The adherent cells were cultured in 1640 culture solution containing 10% fetal bovine serum, 1000 U/ml cytokine rhGM-CSF, and 4500 U/ml rhIL. Half of the culture solution was exchanged after 3 d and supplemented with rhGM-CSF and rhIL-4. After 5 d of culture, the cells were divided into two groups. In the control group, 1000 U/ml TNF-α was added to the culture, whereas 1 μg/ml MMPs of NSCs was added to the culture in the experimental group. After induction and culture for 72 h, the maturation of DCs was observed under an inverted light microscope. Partial DCs from both groups were collected, and the expression levels of CD83 and CD86 in DCs were quantitatively measured by RT-PCR and flow cytometry as previously described [27].

DC-CIK cell induction

The density of the cell suspension was adjusted to 1×10^6 cells/ml, and the cells were transferred to a culture flask containing 1000 U/ml IFN-γ and cultured at 37°C and 5% CO_2 for 24 h in medium supplemented with CD3 monoclonal antibody (100 ng/ml) and rhIL-2 (500 U/ml). After 8 d of culture, DCs loaded with MMPs in the experimental group and DCs in the control group were each mixed and co-cultured with CIK cells at a ratio of 1:100. The solution was exchanged every 3 d and supplemented with rhIL-2. The morphology, growth, and proliferation of DC-CIK cells were observed under an inverted light microscope. The cells and super-

natant were collected after 15 d of culture, and the cell survival rate was assessed by Trypan blue staining [28]. Partial DC-CIK cells were collected from each group. The percentages of cells that were $CD3^+$, $CD3^+CD8^+$, $CD3^+CD56^+$, or $CD3^+CD4^+$ were calculated by flow cytometry [29].

The methyl thiazolyl tetrazolium (MTT) assay

The effector cells were divided into the control group (DC-CIK cells not loaded with MMPs) and the experimental group (DC-CIK cells loaded with MMPs). The third generation of stem cells derived from NB1 and NB2 was used as target cells, and the cell concentration was adjusted to 1×10^5 cells/ml. A total of 100 μl of cell suspension was cultured in each well of a 96-well plate for 6 h. When the target cells had attached to the wall, the effector cells (DC-CIK cells) were added to the 96-well plate at an effector/target ratio of 10:1 or 20:1. After co-culture for 48 h, the morphologies of effector and target cells were observed under an inverted light microscope. The killing rate was evaluated with an MTT assay, and the absorbance (A) value was measured at a wavelength of 570 nm. The cell lysis rate was calculated as previously described [30].

Anti-HLA-E antibody treatment

Third-generation stem cells derived from NB1 and NB2 were used as target cells, and the cell concentration was adjusted to 1×10^5/ml. A total of 100 μl of cell concentration was cultured in each well of a 96-well plate and supplemented with the monoclonal antibody TFL-007 [31] at a final concentration of 25 μg/ml. After culture for 6 h, the cells were attached to the wall. DC-CIK cells or DC-CIK cells loaded with MMPs were used as effector cells, and the experimental procedures above were repeated at an effector/target ratio of 20:1.

SiRNA

SiRNA was designed based on the HLA-E mRNA sequence (NM_005516). The target sequence was ATCTCCGAGCAAAAGTCAAATGA (525-547) [32]. The forward primer sequence was 5'-CU-CCGAGCAAAAGUCAAAUGA-3', and the reverse primer sequence was 5'-AUUUGACUUUUGCU-CGGAGAU-3'. Stem cells derived from NB1 and NB2 that expressed high levels of HLA-E were plated in a 24-well plate at a density of 5×10^4 cell/well, cultured for 18 h, and transfected with 50 pmol siRNA and 2.5 μl Lipofecta-mine 2000 in a total volume of 0.5 ml as previously described [33]. NSCs in which HLA-E was down-regulated were defined as NSCs1-E^{low} and NSCs2-E^{low} cells. For the controls, siRNA was substituted with PBS and nonspecific siRNA.

Statistical analysis

The SPSS 12.0 statistical software was used for data analysis. All data are expressed as the mean ± standard deviation (x ± s). Multi-group comparisons were conducted using a one-way ANOVA. The mean values among groups were statistically compared using *t*-tests. The level of significance was set at α = 0.05, and a *P* value < 0.05 was considered to indicate statistical significance.

Results

NSCs exhibited suspension growth and cell sphere formation

First, NGCs were obtained using a suspension culture method, and their morphology was observed under a light microscope. NB1 and NB2 cells attached to the wall and grew in a short shuttle shape at the bottom of a culture flask containing serum. When cultured for 24 h in a medium without serum, partial suspension cells formed circular clones. After 3 d of culture, a large quantity of cell spheres consisted of dozens of round cells. When the spheres were separated into a single-cell suspension, the passaged cells formed new cell spheres. The cells in the sphere were closely connected, and the cell spheres were robust and exhibited high refraction (**Figure 1A**).

NSCs expressed molecular biomarkers of neural stem cells

To identify whether the cells in the sphere were neural stem cells, immunofluorescence and RT-PCR were employed to measure the expression levels of the differentiation-associated biomarkers nestin, GFAP, and Tuj-1 in tumor cells. Immunofluorescence revealed that cell spheres cultured in serum-free medium highly expressed nestin, whereas the expression of nestin was low in cells cultured in medium containing serum (**Figure 1B**). The protein (**Figure 1C**) and
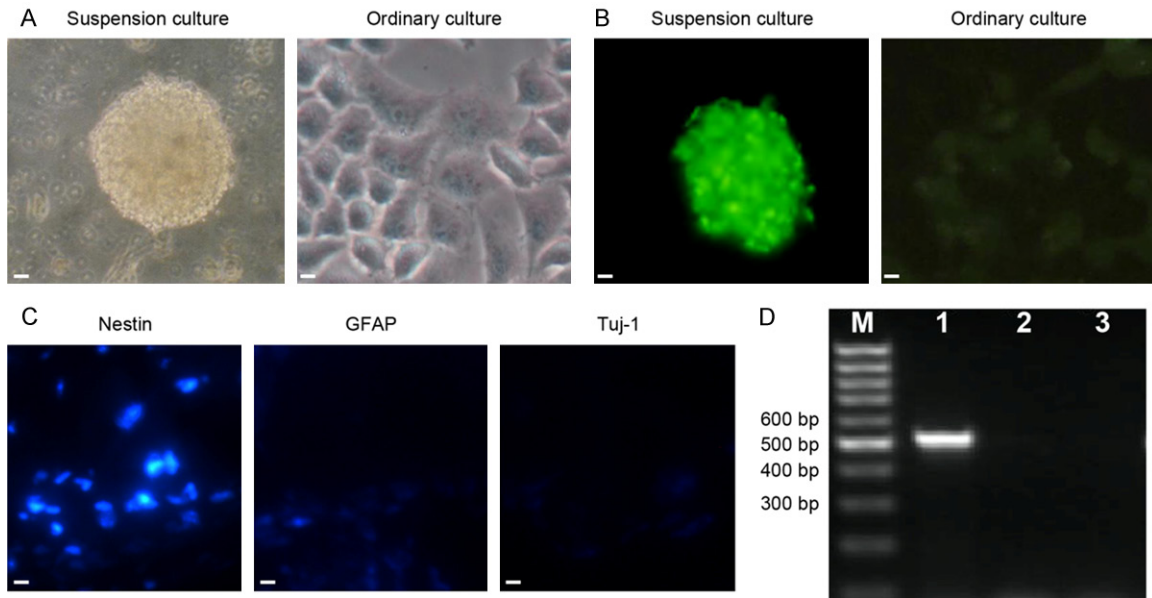
Figure 1. Neuroblastoma stem cells obtained by suspension culture. A. Morphology of cells in suspension culture and common culture observed under light microscopy. Cell spheres formed in suspension culture were robust with high refraction. B. Immunofluorescence showing that cell spheres highly expressed nestin compared to the common culture. C. Immunofluorescence showing nestin was highly expressed in cells from the spheres, whereas the expression of GFAP and Tuj-1 was low or non-existent. D. RT-PCR detection of neural differentiation-associated markers showed nestin, but not GFAP and Tuj-1, was expressed in cells from the spheres. M: marker; 1: Nestin; 2: GFAP; 3: Tuj-1. The data are representative of five independent experiments. All micrographs were captured at 400 × magnification. The scale bar denotes 10 μm.

mRNA (**Figure 1D**) expression levels of nestin, GFAP, and Tuj-1 were further compared, and nestin was highly expressed in cells from the spheres, whereas the expression of GFAP and Tuj-1 was low or even non-existent. Cells from the spheres retained their stem cell status and did not differentiate into gliocytes or neurons.

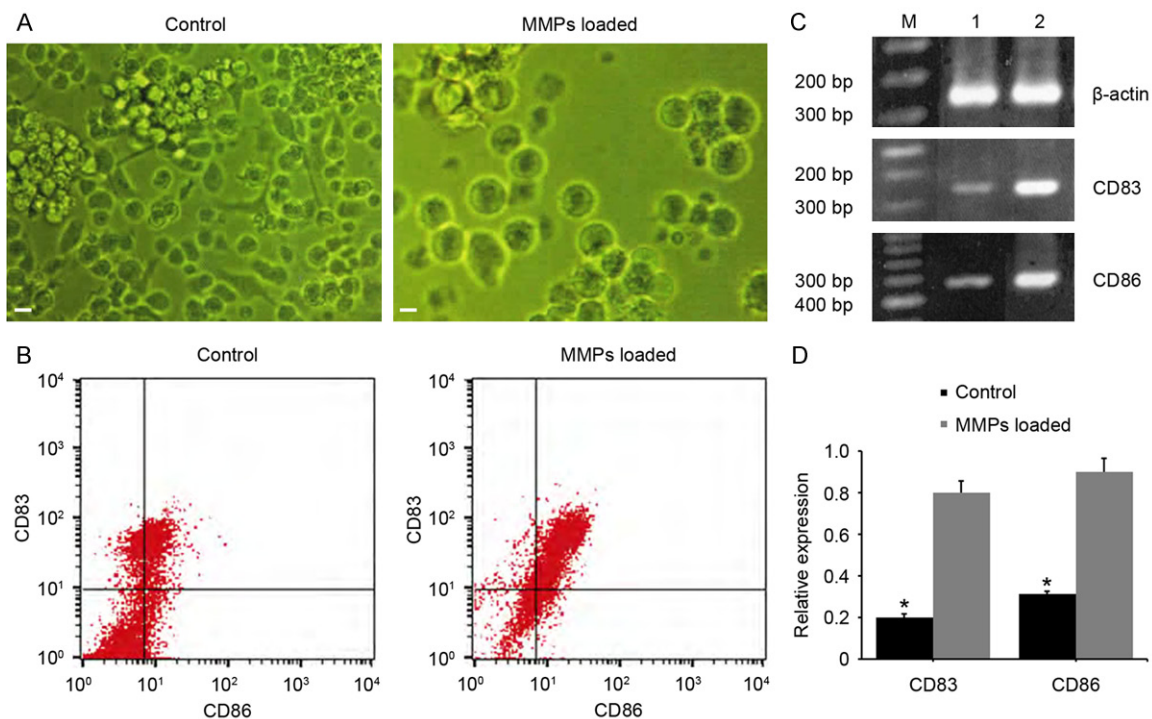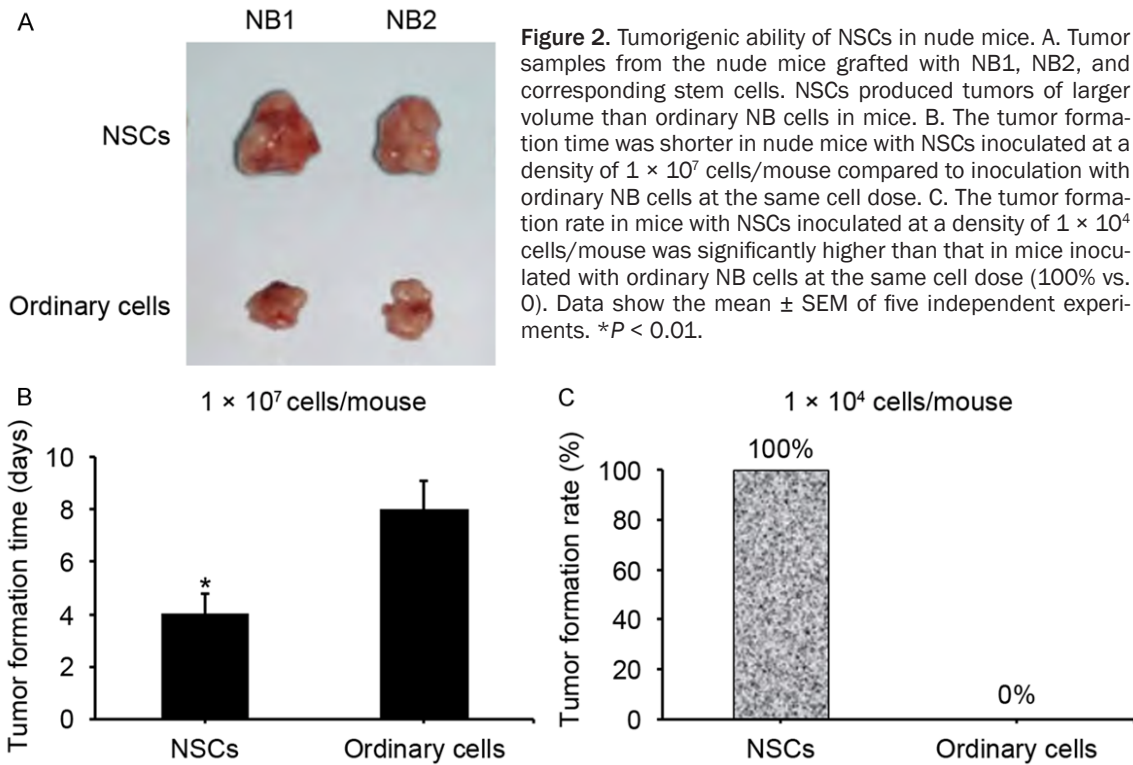*NSCs possessed strong tumorigenic ability in nude mice*

To evaluate the tumorigenicity of NSCs, the tumor formation time and rate in nude mice were compared between NB cells and their counterparts from the cell spheres. When the NSCs derived from NB1 and NB2 cells were subcutaneously inoculated into nude mice at a density of 1×10^7 cells/mouse, tumor formation was observed 3-5 d after inoculation, and the tumor formation rate was 100%. When an equivalent quantity of ordinary NB cells was inoculated, the tumor formation was delayed to 7-9 d after inoculation, but the tumor formation rate remained the same at 100% (**Figure 2A and 2B**). However, when the NSCs were subcutaneously inoculated into the nude mice at a density of 1×10^4 cells/mouse, tumor forma-

tion was evident in all mice after 2 weeks, whereas no significant tumor formation was observed when an equivalent quantity of ordinary cells was inoculated (**Figure 2C**). Thus, the tumorigenicity of NSCs was relatively strong in nude mice.

NSC-derived MMPs induced differentiation of DCs

To load the MMPs into DCs, NSC-derived MMPs were extracted using ultrafiltration and differential centrifugation methods to induce DC differentiation. After being loaded with MMPs for 70 h, DCs exhibited increased volume and a tree root-like bulge in the cytoplasm. The granules became thickened and suspended, which significantly differed from the appearance of DCs that had not been loaded with MMPs (**Figure 3A**). Flow cytometry revealed that the co-expression rate of CD83 and CD86 on the cell surface of DCs was 82.7% ± 4.5% in the experimental group, significantly higher than the 48.3% ± 4.5% rate in the control group (**Figure 3B**). RT-PCR showed that the expression levels of CD83 and CD86 in DCs at the RNA level were up-regulated in the experimen-

Figure 2. Tumorigenic ability of NSCs in nude mice. A. Tumor samples from the nude mice grafted with NB1, NB2, and corresponding stem cells. NSCs produced tumors of larger volume than ordinary NB cells in mice. B. The tumor formation time was shorter in nude mice with NSCs inoculated at a density of 1×10^7 cells/mouse compared to inoculation with ordinary NB cells at the same cell dose. C. The tumor formation rate in mice with NSCs inoculated at a density of 1×10^4 cells/mouse was significantly higher than that in mice inoculated with ordinary NB cells at the same cell dose (100% vs. 0). Data show the mean ± SEM of five independent experiments. *$P < 0.01$.

Figure 3. DC differentiation induced by NSC-derived MMPs. A. Morphology of DCs in the presence and absence of MMPs. B. Flow cytometry showing that the co-expression level of CD83 and CD86 on the cell surface of DCs loaded with NSC-derived MMPs was higher than that on DCs that had not been loaded with MMPs. C. RT-PCR showed that the expression of CD83 and CD86 in DCs at the RNA level was up-regulated in DCs loaded with NSC-derived MMPs. M: marker; 1: DCs without MMPs loaded; 2: DCs with MMPs loaded; β-actin: endogenous control. D. Relative expression of CD83 and CD86 at the RNA level in DCs with or without NSC-derived MMPs loaded. Data show the mean ± SEM of five independent experiments. All micrographs were captured at 400 × magnification. The scale bar denotes 10 μm. *$P < 0.001$.
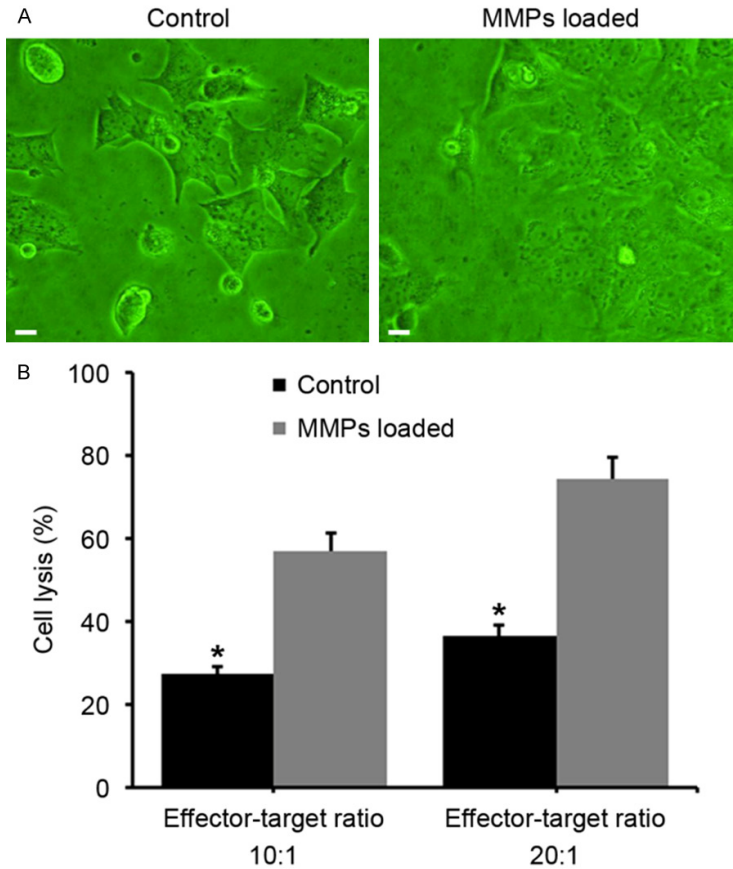
Figure 4. Ability of DC-CIK cells loaded with NSC-derived MMPs to kill NSCs. A. Morphology of NSCs under DC-CIK cell attack. After co-culture with DC-CIK cells loaded with NSC-derived MMPs for 48 h, NSCs exhibited an abnormal cell morphology and morphological changes typical of apoptosis. B. The MTT assay revealed that the cell lysis rate of NSCs was higher when under the attack of DC-CIK cells loaded with NSC-derived MMPs than when under the attack of the same cells that had not been loaded with MMPs. Data show the mean ± SEM of five independent experiments. All micrographs were captured at 400 × magnification. The scale bar denotes 10 μm. *P < 0.01.

culture, the proliferation rate increased, and the cells grew in an irregular cluster shape after 10 d of culture. The survival rate of live cells exceeded 97%, as detected by Trypan blue staining. In the experimental group, the total quantity of DC-CIK cells was increased by 68.5 ± 7.3-fold, significantly higher than the 40.9 ± 4.6-fold increase in the control group. In both groups, partial cells were collected after 15 d of DC and CIK cell co-culture. The cell markers CD3, CD4, CD8, and CD56 were detected by flow cytometry. The phenotype of CD3$^+$CD8$^+$ and CD3$^+$CD56$^+$ in DC-CIK cells loaded with MMPs significantly differed from that of the control (**Table 1**).

The killing of NSCs by DC-CIK cells was enhanced by loading cells with NSC-derived MMPs

DC-CIK cells loaded with NSC-derived MMPs were co-cultured with NSCs from NB1 or NB2 cells. The ability of DC-CIK cells to kill target cells was evaluated with an MTT assay. After culture for 48 h, an abnormal cell morphology, including cell fragmentation and nucleus exposure, was observed in target cells under DC-CIK cell attack. Moreover, typical morphological changes related to apoptosis, such as nuclear chromatin aggregation, karyorrhexis, and cytoplasm condensation, were present (**Figure 4A**). The MTT assay revealed that the ability of DC-CIK cells loaded with MMPs at an effector/target ratio of 10:1 or 20:1 to kill NSCs was significantly higher than that of the control group (**Figure 4B**).

Inhibition of HLA-E enhanced the function of DC-CIK cells loaded with NSC-derived MMPs

To evaluate the effect of HLA-E on DC-CIK cell function, the expression and function of HLA-E in NSCs from NB1 and NB2 cells was inhibited. The ability of DC-CIK cells loaded with NSC-derived MMPs to kill target cells was assessed

tal group (**Figure 3C** and **3D**). Thus, NSC-derived MMPs were able to induce the maturation of DCs.

NSC-derived MMPs induced the differentiation of DC-CIK cells

To obtain DC-CIK cells that target and kill NB1 and NB2 cells, DCs and CIK cells loaded with NSC-derived MMPs were mixed and cultured, and the immunophenotypes of cells were assessed by flow cytometry. Compared to the cells that had not been loaded with MMPs, DC-CIK cells loaded with MMPs rapidly proliferated after 3 d of mixed culture, and the cell body was enlarged (**Figure 4A**). After 5-6 d of

Table 1. Immunophenotype of DC-CIK cells loaded with NSC-derived MMPs

Tumor cell	Group	Immunophenotype			
		CD3$^+$	CD3$^+$CD56$^+$	CD3$^+$CD8$^+$	CD3$^+$CD4$^+$
NB1	MMPs loaded	74.1 ± 7.1	15.2 ± 5.8	19.8 ± 6.3	13.6 ± 4.5
	No MMPs loaded	75.6 ± 8.9	69.3 ± 9.8*	73 ± 8.2*	12.8 ± 3.9
NB2	MMPs loaded	72.6 ± 6.5	14.5 ± 6.1	18.9 ± 5.4	11.9 ± 3.8
	No MMPs loaded	71.5 ± 5.6	70.3 ± 7.3*	71 ± 6.7*	12.3 ± 4.1

*all $P < 0.001$ vs. MMPs loaded.

with an MTT assay. The combined use of DC-CIK cells and HLA-E monoclonal antibody significantly enhanced the killing effect of DC-CIK cells. This improvement was maximized when HLA-E monoclonal antibody was used in combination with DC-CIK cells loaded with NSC-derived MMPs (**Figure 5A**).

To verify that the effect of HLA-E monoclonal antibody on the function of DC-CIK cells was mediated by the inhibition of HLA-E, the expression of HLA-E in NSCs was down-regulated by siRNA, and the ability of DC-CIK cells to kill NSCs was re-assessed. Fluorescent quantitative RT-PCR revealed that HLA-E was not expressed in NSCs1-E^{low} or NSCs2-E^{low} cells. The HLA-E gene was completely silenced (**Figure 5B**). The ability of DC-CIK cells to target and kill NSCs-E^{low} cells was significantly higher than that of cells in which HLA-E was not down-regulated. Moreover, the ability of DC-CIK cells to kill NSCs in which HLA-E down-regulated was maximized when DC-CIK cells were loaded with MMPs (**Figure 5C**).

Finally, the combined effect of down-regulating HLA-E expression in target cells and using HLA-E monoclonal antibody was investigated. The ability of DC-CIK cells loaded with NSC-derived MMPs to kill NSCs-E^{low} remained high, but use of HLA-E monoclonal antibody failed to further enhance this capability. Both HLA-E monoclonal antibody and the down-regulation of HLA-E expression in NSCs similarly enhanced the cell lysis of NSCs by DC-CIK cells loaded with MMPs (**Figure 5D**).

Discussion

In this study, NB stem cells were successfully obtained using a suspension culture method. The growth characteristics of NB stem cells differed from those of ordinary NB cells both *in vitro* and *in vivo*. Similar cells exhibiting the characteristics of stem cells were first identified in breast cancer [34]; these cells exhibited self-renewal, multi-differentiation, and strong tumorigenic ability, defining them as tumor stem cells. Subsequently, tumor stem cells have been identified in multiple adult tumors [35, 36] and have been suggested to be the seeding cells of malignant tumors and play a critical role in the recurrence and metastasis of tumors [37, 38]. In this study, we successfully isolated stem cells from NB, which might contribute to changing conventional knowledge of NB and provide a new approach to NB treatment [39].

Multiple detection methods were applied to identify the characteristics of stem cells within cell spheres obtained by suspension culture, which demonstrated that nestin was highly expressed in these cells. Nestin is a specific antigen of nerve epithelial cells, and its expression level gradually decreases as nerve cells differentiate, a change that has been widely applied to identify neural stem cells [40]. The expression of the astrocyte markers GFAP and Tuj-1 was low or non-existent, suggesting that the cells inside the cell spheres retained their stem-cell status and did not differentiate into gliocytes or neurons. *In vivo* studies further demonstrated that the tumorigenicity of NSCs was significantly higher than that of ordinary NB cells. NSCs exhibit directional differentiation, high self-proliferation and even malignant biological behavior compared to ordinary NB cells. Similar to multiple adult tumors [41-43], the elimination of NSCs contributes to the success of NB treatment.

At a time when conventional modalities, such as chemotherapy, surgery, and radiotherapy, cannot readily yield further breakthroughs in NB treatment, an effective immunotherapy may provide a new treatment direction [44-46]. In this study, NSC-derived MMPs, a novel category of antigen, were loaded onto DCs to endow them with specific anti-tumor immunity for NSCs. NSC-derived MMPs carry the specific antigens expressed in parent cells. Loading DCs with MMPs sensitized DCs and up-regulated the DC maturation-associated markers CD83 and CD86. In recent years, multiple sources of
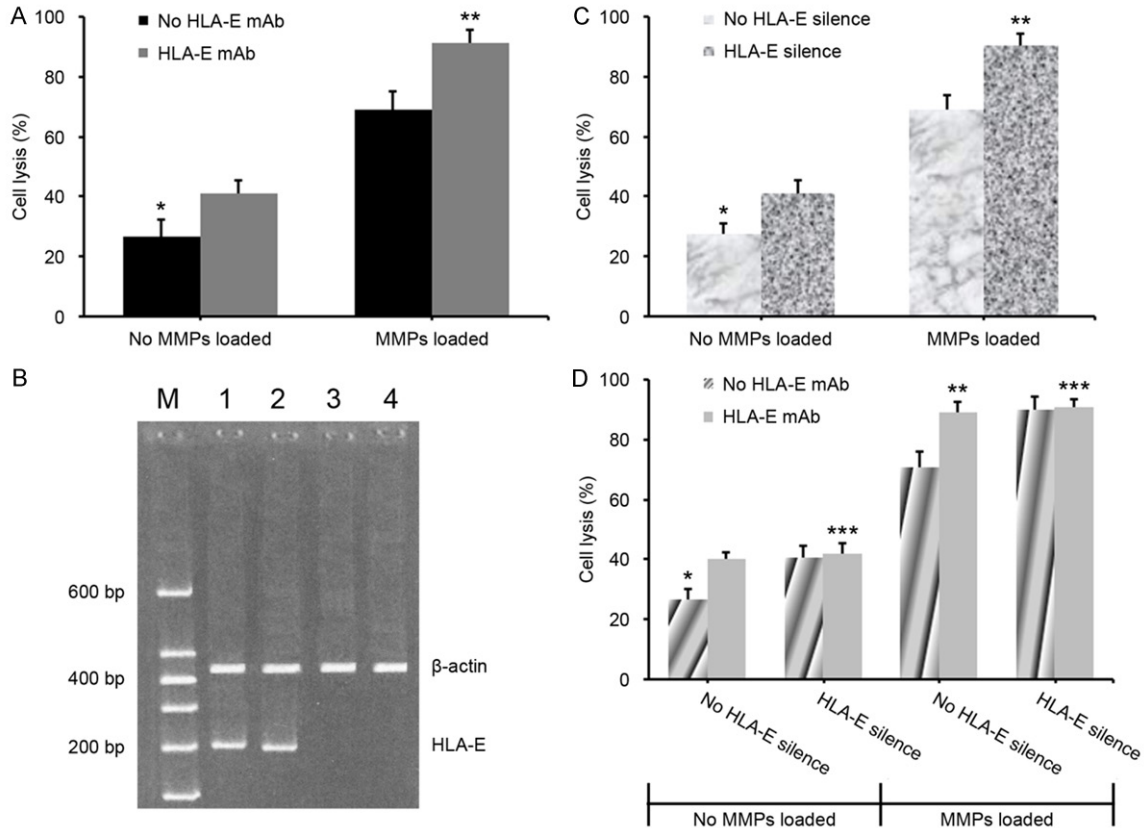
Figure 5. Effect of HLA-E inhibitor on the function of DC-CIK cells loaded with NSC-derived MMPs. A. Cell lysis rate of NSCs co-cultured with DC-CIK cells or DC-CIK cells loaded with NSC-derived MMPs in the presence or absence of HLA-E monoclonal antibody. B. Fluorescent quantitative RT-PCR revealed that the HLA-E gene was completely silenced in NSCs. M: marker; 1: blank control; 2: nonspecific siRNA control; 3: NSCs derived from NB1 cells; 4: NSCs derived from NB2 cells; β-actin: endogenous. C. Cell lysis rate of NSCs co-cultured with DC-CIK cells or DC-CIK cells loaded with NSC-derived MMPs in the presence or absence of HLA-E gene silencing. D. Combined effect of HLA-E monoclonal antibody and down-regulation of HLA-E expression in NSCs on the cell lysis of NSCs by DC-CIK cells in the presence of absence of NSC-derived MMP loading. mAb: monoclonal antibody. Data show the mean ± SEM of five independent experiments. *$P < 0.05$; **$P < 0.001$; ***$P > 0.05$.

tumor complete antigens have been reported, such as exposing tumor cells to radiation, tumor cell lysate, tumor cell-derived RNA, and apoptotic bodies [13, 47]. DCs loaded with complete antigens were able to induce a polyvalent immunoreaction, likely via MHC-I and MHC-II antigen-presenting pathways, and amplify immunological reactivity by inducing a synergistic effect between specific CTL and Th cells.

To obtain specific CTLs for NSCs, DCs loaded with NSC-derived MMPs were co-cultured with CIK cells. Flow cytometry showed that the percentage of CD3+CD8+ and CD3+CD56+ double-positive cells was significantly higher among DC-CIK cells loaded with NSC-derived MMPs than among cells that had not been loaded with MMP. This increase significantly enhanced the

ability of DC-CIK cells to kill and target NSCs *in vitro*. These results suggest that NSC-derived MMPs are likely to adhere to DCs and induce endocytosis. NSC-derived MMPs can be processed and presented to CIK cells by DCs, thereby activating their specific recognition and killing. Additionally, we found that co-culturing DCs loaded with NSC-derived MMPs and CIK cells enhanced the proliferation rate of CIK cells, which might contribute to the ability of DC-CIKs to counteract adverse events in the tumor microenvironment [48] and exert a successful anti-tumor effect when further used *in vivo*.

Atypical HLA-I molecules on the tumor cell surface can assist in the immunologic escape of malignant tumors and present a barrier to immunotherapy against tumors [17]. To over-

come the effect of HLA-E expressed in NSCs on DC-CIK cell function, HLA-E monoclonal antibody was supplemented when DC-CIK cells were applied to kill NSCs. DC-CIK cells further enhanced the cell lysis rate of target cells by approximately 90%. The effect of HLA-E monoclonal antibody on the anti-tumor function of DC-CIK cells was consistent with the HLA-E gene silencing of target cells. HLA-E monoclonal antibody blocked the binding between tumor cell-derived HLA-E and inhibitory receptors on CIK cells and enhanced the cytolytic activity of $CD3^+CD56^+T$ cells and other effector cells. This synergistic effect of DC-CIK cells in combination with HLA-E monoclonal antibody might contribute to decrease the quantity of infused immunocytes without compromising the anti-tumor effect, thus reducing the side effects of immunotherapy when applied *in vivo* [49, 50].

HLA-G, another atypical HLA-I molecule, was not investigated in the present study. HLA-G is highly expressed in multiple tumors, including NB [51]. Moreover, HLA-G can inhibit the activity of NK cells and CTLs to assist tumors in escaping from immune killing. Nevertheless, HLA-G cannot directly bind with CD94/NKG2A, whereas the leading peptide of HLA-G binds with HLA-E to form a complex that activates the CD94/NKG2A receptor, which transmits the inhibiting signal [52]. In a recent study, a proteomic comparison was adopted to analyze 363 categories of proteins in glioma, which demonstrated that the inhibitory effect of tumor cells on immunocytes was mediated by HLA-E [53]. Thus, HLA-G expressed in NSCs may not affect the current results.

In conclusion, HLA-E inhibitor can enhance the ability of DC-CIK cells loaded with NSC-derived MMPs to target and kill NSCs. In future practice, conventional treatment may be used to minimize the tumor burden of NB patients, followed by therapy with DC-CIK cells loaded with NSC-derived MMPs in combination with HLA-E monoclonal antibody to eliminate NSCs. This novel modality may decrease the recurrence of NB, a possibility that deserves further investigation.

Acknowledgements

Disclosure of conflict of interest

None.

Abbreviations

NB, neuroblastoma; NSCs, neuroblastoma stem cells; DCs, dendritic cells; CIK, cytokine-induced killer; MMPs, membrane-based microparticles; HLA-E, human leukocyte antigen-E; NK, natural killer; CTLs, cytotoxic T lymphocytes; PBS, phosphate-buffered saline; RT-PCR, reverse transcription-polymerase chain reaction; GFAP, glial fibrillary acid protein; MTT, methyl thiazolyl tetrazolium.

Address correspondence to: Dr. Zijun Zhen, Department of Pediatric Oncology, Sun Yat-sen University Cancer Center, 651 Dongfeng Road East, Guangzhou 510060, China. Tel: (86) 20-87342468; Fax: (86) 20-87343694; E-mail: zhenzj@sysucc.org.cn

References

[1] Cheung NK, Cheung IY, Kushner BH, Ostrovnaya I, Chamberlain E, Kramer K, Modak S. Murine anti-GD2 monoclonal antibody 3F8 combined with granulocyte-macrophage colony-stimulating factor and 13-cis-retinoic acid in high-risk patients with stage 4 neuroblastoma in first remission. J Clin Oncol 2012; 30: 3264-3270.

[2] Kreissman SG, Seeger RC, Matthay KK, London WB, Sposto R, Grupp SA, Haas-Kogan DA, Laquaglia MP, Yu AL, Diller L, Buxton A, Park JR, Cohn SL, Maris JM, Reynolds CP, Villablanca JG. Purged versus non-purged peripheral blood stem-cell transplantation for high-risk neuroblastoma (COG A3973): a randomised phase 3 trial. Lancet Oncol 2013; 14: 999-1008.

[3] Kasai T, Chen L, Mizutani A, Kudoh T, Murakami H, Fu L, Seno M. Cancer stem cells converted from pluripotent stem cells and the cancerous niche. J Stem Cells Regen Med 2014; 10: 2-7.

[4] Garner EF, Beierle EA. Cancer stem cells and their interaction with the tumor microenvironment in neuroblastoma. Cancers (Basel) 2015; 8.

[5] Forgham H, Johnson D, Carter N, Veuger S, Carr-Wilkinson J. Stem cell markers in neuroblastoma-an emerging role for LGR5. Front Cell Dev Biol 2015; 3: 77.

[6] He S, Yin T, Li D, Gao X, Wan Y, Ma X, Ye T, Guo F, Sun J, Lin Z, Wang Y. Enhanced interaction between natural killer cells and lung cancer cells: involvement in gefitinib-mediated immunoregulation. J Transl Med 2013; 11: 186.

[7]   Mei JZ, Liu GJ, Zhang XJ, Zhao JZ, Feng RT. Erlotinib enhances the CIK cell-killing sensitivity of lung adenocarcinoma A549 cells. Genet Mol Res 2015; 14: 3082-3089.

[8]   Yu X, Zhao H, Liu L, Cao S, Ren B, Zhang N, An X, Yu J, Li H, Ren X. A randomized phase II study of autologous cytokine-induced killer cells in treatment of hepatocellular carcinoma. J Clin Immunol 2014; 34: 194-203.

[9]   Chen R, Deng X, Wu H, Peng P, Wen B, Li F, Li F. Combined immunotherapy with dendritic cells and cytokine-induced killer cells for malignant tumors: a systematic review and meta-analysis. Int Immunopharmacol 2014; 22: 451-464.

[10] Giraudo L, Gammaitoni L, Cangemi M, Rotolo R, Aglietta M, Sangiolo D. Cytokine-induced killer cells as immunotherapy for solid tumors: current evidence and perspectives. Immunotherapy 2015; 7: 999-1010.

[11] Wang YF, Kunda PE, Lin JW, Wang H, Chen XM, Liu QL, Liu T. Cytokine-induced killer cells cocultured with complete tumor antigen-loaded dendritic cells, have enhanced selective cytotoxicity on carboplatin-resistant retinoblastoma cells. Oncol Rep 2013; 29: 1841-1850.

[12] Mignot G, Roux S, Thery C, Ségura E, Zitvogel L. Prospects for exosomes in immunotherapy of cancer. J Cell Mol Med 2006; 10: 376-388.

[13] Hao S, Moyana T, Xiang J. Review: cancer immunotherapy by exosome-based vaccines. Cancer Biother Radiopharm 2007; 22: 692-703.

[14] Baj-Krzyworzeka M, Szatanek R, Weglarczyk K, Baran J, Urbanowicz B, Brański P, Ratajczak MZ, Zembala M. Tumour-derived microvesicles carry several surface determinants and mRNA of tumour cells and transfer some of these determinants to monocytes. Cancer Immunol Immunother 2006; 55: 808-818.

[15] Petrie EJ, Clements CS, Lin J, Sullivan LC, Johnson D, Huyton T, Heroux A, Hoare HL, Beddoe T, Reid HH, Wilce MC, Brooks AG, Rossjohn J. CD94-NKG2A recognition of human leukocyte antigen (HLA)-E bound to an HLA class I leader sequence. J Exp Med 2008; 205: 725-735.

[16] Morandi F, Pozzi S, Carlini B, Amoroso L, Pistoia V, Corrias MV. Soluble HLA-G and HLA-E Levels in bone marrow plasma samples are related to disease stage in neuroblastoma patients. J Immunol Res 2016; 2016: 7465741.

[17] Zhen Z, Guo X, Liao R, Yang K, Ye L, You Z. Involvement of IL-10 and TGF-β in HLA-E-mediated neuroblastoma migration and invasion. Oncotarget 2016; 7: 44340-44349.

[18] Cao J, Chen C, Wang Y, Chen X, Chen Z, Luo X. Influence of autologous dendritic cells on cytokine-induced killer cell proliferation, cell phenotype and antitumor activity in vitro. Oncol Lett 2016; 12: 2033-2037.

[19] Mingari MC, Moretta A, Moretta L. Regulation of KIR expression in human T cells: a safety mechanism that may impair protective T-cell responses. Immunol Today 1998; 19: 153-157.

[20] World Medical Association. World Medical Association Declaration of Helsinki: ethical principles for medical research involving human subjects. World Medical Association. JAMA 2013; 310: 2191-2194.

[21] Chaban VV, Cho T, Reid CB, Norris KC. Physically disconnected non-diffusible cell-to-cell communication between neuroblastoma SH-SY5Y and DRG primary sensory neurons. Am J Transl Res 2013; 5: 69-79.

[22] Ishigami S, Arigami T, Okumura H, Uchikado Y, Kita Y, Kurahara H, Maemura K, Kijima Y, Ishihara Y, Sasaki K, Uenosono Y, Natsugoe S. Human leukocyte antigen (HLA)-E and HLA-F expression in gastric cancer. Anticancer Res 2015; 35: 2279-2285.

[23] Bueno-Sánchez JC, Peña-Alzate S, Peña RB, Agudelo-Jaramillo B, Cadavid-Jaramillo AP, Chaouat G, Maldonado-Estrada JG. Sera from early-onset, severely preeclamptic women directly modulate HLA-E expression in the EA.hy-296 endothelial cell line. J Reprod Immunol 2014; 104-105: 68-79.

[24] Tseng CN, Hong YR, Chang HW, Yu TJ, Hung TW, Hou MF, Yuan SS, Cho CL, Liu CT, Chiu CC, Huang CJ. Brefeldin A reduces anchorage-independent survival, cancer stem cell potential and migration of MDA-MB-231 human breast cancer cells. Molecules 2014; 19: 17464-17477.

[25] Coculova M, Imrichova D, Seres M, Messingerova L, Bohacova V, Sulova Z, Breier A. The expression of P-glycoprotein in leukemia cells is associated with the upregulated expression of nestin, a class 6 filament protein. Leuk Res 2016; 48: 32-39.

[26] Baj-Krzyworzeka M, Szatanek R, Weglarczyk K, Baran J, Urbanowicz B, Brański P, Ratajczak MZ, Zembala M. Tumour-derived microvesicles carry several surface determinants and mRNA of tumour cells and transfer some of these determinants to monocytes. Cancer Immunol Immunother 2006; 55: 808-818.

[27] Jagessar SA, Vierboom M, Blezer EL, Bauer J, Hart BA, Kap YS. Overview of models, methods, and reagents developed for translational autoimmunity research in the common marmoset (Callithrix jacchus). Exp Anim 2013; 62: 159-171.

[28] Li GX, Zhao SS, Zhang XG, Wang WH, Liu J, Xue KW, Li XY, Guo YX, Wang LH. Comparison of the proliferation, cytotoxic activity and cytokine secretion function of cascade primed immune cells and cytokine-induced killer cells in vitro. Mol Med Rep 2015; 12: 2629-2635.

[29] Wang L, Yi Y, Yin D, Zhou Z, Fan J, Ye W, Zhao W. Augmented CD3(+)CD8(+) and CD3(+)CD56(-) cells in cytokine-induced killer cells

cultured with engineered cells for costimulatory enhancement from heavily pretreated patients with solid tumor. Cytotherapy 2016; 18: 581-589.

[30] Chatzopoulou EI, Roskopf CC, Sekhavati F, Braciak TA, Fenn NC, Hopfner KP, Oduncu FS, Fey GH, Rädler JO. Chip-based platform for dynamic analysis of NK cell cytolysis mediated by a triplebody. Analyst 2016; 141: 2284-2295.

[31] Ravindranath MH, Terasaki PI, Pham T, Jucaud V, Kawakita S. Therapeutic preparations of IVIg contain naturally occurring anti-HLA-E Abs that react with HLA-Ia (HLA-A/-B/-Cw) alleles. Blood 2013; 121: 2013-2028.

[32] Ui-Tei K, Naito Y, Takahashi F, Haraguchi T, Ohki-Hamazaki H, Juni A, Ueda R, Saigo K. Guidelines for the selection of highly effective siRNA sequences for mammalian and chick RNA interference. Nucleic Acids Res 2004; 32: 936-948.

[33] Lee S, Qiao J, Paul P, Chung DH. Integrin β1 is critical for gastrin-releasing peptide receptor-mediated neuroblastoma cell migration and invasion. Surgery 2013; 154: 369-375.

[34] Al-Hajj M, Wicha MS, Benito-Hernandez A, Morrison SJ, Clarke MF. Prospective identification of tumorigenic breast cancer cells. Proc Natl Acad Sci U S A 2003; 100: 3983-3988.

[35] Singh SK, Clarke ID, Terasaki M, Bonn VE, Hawkins C, Squire J, Dirks PB. Identification of a cancer stem cell in human brain tumors. Cancer Res 2003; 63: 5821-5828.

[36] Lam JS, Reiter RE. Stem cells in prostate and prostate cancer development. Urol Oncol 2006; 24: 131-140.

[37] Easwaran H, Tsai HC, Baylin SB. Cancer epigenetics: tumor heterogeneity, plasticity of stem-like states, and drug resistance. Mol Cell 2014; 54: 716-727.

[38] Jernberg Wiklund H, Westermark B. Taming the cancer cell. J Intern Med 2014; 276: 2-4.

[39] Diede SJ. Spontaneous regression of metastatic cancer: learning from neuroblastoma. Nat Rev Cancer 2014; 14: 71-72.

[40] MacDonald TJ, Aguilera D, Castellino RC. The rationale for targeted therapies in medulloblastoma. Neuro Oncol 2014; 16: 9-20.

[41] Jung JG, Shih IM, Park JT, Gerry E, Kim TH, Ayhan A, Handschuh K, Davidson B, Nickles Fader A, Selleri L, Wang TL. Ovarian cancer chemoresistance relies on the stem cell reprogramming factor PBX1. Cancer Res 2016; 76: 6351-6361.

[42] Li Q, Wei P, Huang B, Xu Y, Li X, Li Y, Cai S, Li D. MAEL expression links epithelial-mesenchymal transition and stem cell properties in colorectal cancer. Int J Cancer 2016; 139: 2502-2511.

[43] Shah K. Stem cell-based therapies for tumors in the brain: are we there yet? Neuro Oncol 2016; 18: 1066-1078.

[44] Cappel C, Huenecke S, Suemmerer A, Erben S, Rettinger E, Pfirrmann V, Heinze A, Zimmermann O, Klingebiel T, Ullrich E, Bader P, Bremm M. Cytotoxic potential of IL-15-activated cytokine-induced killer cells against human neuroblastoma cells. Pediatr Blood Cancer 2016; 63: 2230-2239.

[45] Singh N, Kulikovskaya I, Barrett DM, Binder-Scholl G, Jakobsen B, Martinez D, Pawel B, June CH, Kalos MD, Grupp SA. T cells targeting NY-ESO-1 demonstrate efficacy against disseminated neuroblastoma. Oncoimmunology 2015; 5: e1040216.

[46] Cordeau M, Belounis A, Lelaidier M, Cordeiro P, Sartelet H, Herblot S, Duval M. Efficient killing of high risk neuroblastoma using natural killer cells activated by plasmacytoid dendritic cells. PLoS One 2016; 11: e0164401.

[47] Mignot G, Roux S, Thery C, Ségura E, Zitvogel L. Prospects for exosomes in immunotherapy of cancer. J Cell Mol Med 2006; 10: 376-88.

[48] Giraudo L, Gammaitoni L, Cangemi M, Rotolo R, Aglietta M, Sangiolo D. Cytokine-induced killer cells as immunotherapy for solid tumors: current evidence and perspectives. Immunotherapy 2015; 7: 999-1010.

[49] Resetca D, Neschadim A, Medin JA. Engineering hematopoietic cells for cancer immunotherapy: strategies to address safety and toxicity concerns. J Immunother 2016; 39: 249-259.

[50] Tanaka T, Narazaki M, Kishimoto T. Immunotherapeutic implications of IL-6 blockade for cytokine storm. Immunotherapy 2016; 8: 959-970.

[51] Morandi F, Scaruffi P, Gallo F, Stigliani S, Moretti S, Bonassi S, Gambini C, Mazzocco K, Fardin P, Haupt R, Arcamone G; Italian Cooperative Group for Neuroblastoma, Pistoia V, Tonini GP, Corrias MV. Bone marrow-infiltrating human neuroblastoma cells express high levels of calprotectin and HLA-G proteins. PLoS One 2012; 7: e29922.

[52] Brooks AG, Borrego F, Posch PE, Patamawenu A, Scorzelli CJ, Ulbrecht M, Weiss EH, Coligan JE. Specific recognition of HLA-E, but not classical, HLA class I molecules by soluble CD94/NKG2A and NK cells. J Immunol 1999; 162: 305-313.

[53] He W, Kuang Y, Xing X, Simpson RJ, Huang H, Yang T, Chen J, Yang L, Liu E, He W, Gu J. Proteomic comparison of 3D and 2D glioma models reveals increased HLA-E expression in 3D models is associated with resistance to NK cell-mediated cytotoxicity. J Proteome Res 2014; 13: 2272-2281.